Estuarine, Coastal and Shelf Science 142 (2014) 4–11

Contents lists available at ScienceDirect

Estuarine, Coastal and Shelf Science

journal homepage: www.elsevier.com/locate/ecss

Sulfur and oxygen isotope tracing of sulfate driven anaerobic methane oxidation in estuarine sediments

Gilad Antler [a,*], Alexandra V. Turchyn [a], Barak Herut [b], Alicia Davies [a], Victoria C.F. Rennie [a], Orit Sivan [c]

[a] Department of Earth Sciences, University of Cambridge, Cambridge CB2 3EQ, UK
[b] Israel Oceanographic and Limnological Research, National Institute of Oceanography, Haifa 31080, Israel
[c] Department of Geological and Environmental Sciences, Ben Gurion University, Beer Sheva 84105, Israel

ARTICLE INFO

Article history:
Received 7 November 2013
Accepted 1 March 2014
Available online 13 March 2014

Keywords:
sulfate
methane
estuaries
isotopes
AOM

ABSTRACT

We use multiple stable isotope measurements in two highly stratified estuaries located along the Mediterranean coast of Israel (the Yarqon and the Qishon) to explore the consumption of sulfate through the anaerobic oxidation of methane (sulfate-driven AOM). At both sites, pore fluid sulfate is rapidly consumed within the upper 15–20 cm. Although the pore fluid sulfate and dissolved inorganic carbon (DIC) concentration profiles change over a similar range with respect to depth, the sulfur and oxygen isotopes in the pore fluid sulfate and the carbon isotopes in the pore fluid DIC are fundamentally different. This pore fluid isotope geochemistry indicates that the microbial mechanism of sulfate reduction differs between the studied sites. We suggest that in the Yarqon estuary, sulfate is consumed entirely through AOM, whereas in the Qishon, both AOM and bacterial sulfate reduction through organic matter oxidation coexist. These results have implications for understanding the microbial mechanisms behind sulfate-driven AOM. Our data compilation from marine and marginal marine environments supports the conclusion that the intracellular pathways of sulfate reduction varies among environments with sulfate-driven AOM. The data can be used to elucidate new pathways in the cycling of methane and sulfate, and the findings are applicable to the broader marine environment.

1. Introduction

1.1. General

Organic carbon in marine and marginal marine sediments can be oxidized anaerobically through various electron acceptors (Froelich et al., 1979). These anaerobic electron acceptors are used in order of decreasing chemical potential, beginning with nitrate, and proceeding through manganese and iron oxides, and sulfate (Froelich et al., 1979). Any organic matter that is not oxidized aerobically or anaerobically can undergo further reduction, leading to the formation of methane (CH_4) in the process of methanogenesis (e.g. Whiticar et al., 1986). Marine sediments are the largest natural reservoir of methane on Earth (Kvenvolden, 1988).

Upwardly diffusing methane can be oxidized microbially (methanotrophy), both aerobically (via oxygen—e.g. Cicerone and Oremland, 1988) and anaerobically (anaerobic oxidation of methane —AOM—e.g. Martens and Berner, 1974; Hinrichs et al., 1999; Boetius et al., 2000; Milucka et al., 2012). In marine and marginal marine sediments, AOM has been identified as the main process consuming methane in the subsurface, and this methane oxidation is primarily coupled to sulfate reduction (hereafter called sulfate-driven AOM) (Eq. (1)—e.g. Martens and Berner, 1974; Barnes and Goldberg, 1976; Reeburgh, 1976):

$$SO_4^{2-} + CH_4 \rightarrow HCO_3^- + HS^- + H_2O \quad (1)$$

Sulfate-driven AOM often results in a geochemically detectable transition zone at the boundary between methane diffusing upwardly through the network of sedimentary pore fluids, intersecting with sulfate, diffusing downwardly from the overlying ocean (e.g. Niewöhner et al., 1998). Methane emissions from marine sediments are an order of magnitude smaller than those from rice paddies or terrestrial wetlands because of this sulfate-driven AOM, due to the large concentration of sulfate in the modern ocean (Wuebbles and Hayhoe, 2002). The fact that a high percentage of methane in marine sediments is oxidized through sulfate-driven AOM means that the earth's vast oceans are prevented from

* Corresponding author.
E-mail address: ga307@cam.ac.uk (G. Antler).

http://dx.doi.org/10.1016/j.ecss.2014.03.001
0272-7714/

becoming a major source of this potent greenhouse gas (Reeburgh, 2007).

Sulfate-driven AOM was first identified using evidence from sediment geochemical profiles (Martens and Berner, 1974; Barnes and Goldberg, 1976; Reeburgh, 1976). This process was initially controversial among microbiologists, because neither the responsible organism nor the mechanism was identified. About twenty years ago, field and laboratory studies demonstrated coupling between methanogens and sulfate reducers (Hoehler et al., 1994). Later, microbiologists and geochemists showed that consortia of archaea and bacteria are involved in AOM in some seep environments (Hinrichs et al., 1999; Boetius et al., 2000; Orphan et al., 2001), and that at least three groups of archaea may perform AOM (named ANME-1, ANME-2, and ANME-3) associated with sulfate reducing bacteria (Boetius et al., 2000; Orphan et al., 2002; Niemann et al., 2006). It was suggested that the archaea are responsible for the methane oxidation while the sulfate reducing bacteria separately reduce the sulfate. Recently it was shown that some ANMEs are able to oxidize methane and reduce sulfate alone and the bacteria-archaea consortia may not be required (Milucka et al., 2012).

Some specifics of sulfate-driven AOM and its link to the subsurface sedimentary sulfur cycle, however, remain enigmatic. For instance, if we consider the proposed consortia for sulfate-driven AOM, it is still unclear what drives the coupling between sulfate reducers and methane oxidizers and how this is energetically favorable for each. If we consider, on the other hand, that a single ANME performs both sulfate reduction and methane oxidation (Milucka et al., 2012), we do not yet know how prevalent this is in the natural environment and the role of key intermediate valence sulfur species in this pathway of sulfate-driven AOM. Additionally, sulfate reducing bacteria can oxidize sedimentary organic matter, yet several studies have shown that when methane is present, all available sulfate is reduced through the less energetically favorable pathway of AOM (Niewöhner et al., 1998; Kasten and Jørgensen, 2000; Sivan et al., 2007). The lack of answers to these questions limits our understanding of the subsurface sulfur cycle and the crucial coupling to methanotrophy.

Carbon isotopes provide a good constraint on the depth distribution and location of methanogenesis and methanotrophy because of the large carbon isotopic fractionation associated with both methane production and consumption (e.g. Whiticar, 1999; Borowski et al., 2000). During methanogenesis, ^{12}C is strongly partitioned into methane; the $\delta^{13}C$ of the methane produced can be between −50‰ and −100‰. In contrast, the residual dissolved inorganic carbon pool becomes highly enriched in ^{13}C, occasionally by as much as 50–70‰. Oxidizing this methane during AOM on the other hand, results in ^{13}C-depleted dissolved inorganic carbon (DIC) and slightly heavier $\delta^{13}C$ values of the residual methane, due to both a fractionation of 0–10‰ during methane oxidation and to the initial $\delta^{13}C$ value of the methane itself (Alperin et al., 1988; Martens et al., 1999). Therefore, in sedimentary environments where methane is being produced and consumed, the $\delta^{13}C$ of dissolved inorganic carbon in the pore fluid typically follows a depth profile where it decreases from the surface to the zone of AOM and then increases below in the zone where methane is being produced (e.g. Blair and Aller, 1995; Sivan et al., 2007; Malinverno and Pohlman, 2011).

The sulfur and oxygen isotope ratios in dissolved sulfate in sedimentary pore fluids may also be a powerful tool for studying sulfate-driven AOM. Sulfur isotope fractionation during bacterial sulfate reduction, which partitions ^{32}S into the sulfide leaving ^{34}S behind in the residual sulfate, can be as high as 72‰ (e.g. Wortmann et al., 2001; Brunner and Bernasconi, 2005; Sim et al., 2011). As sulfate is reduced to sulfide via intercellular intermediates (Rees, 1973; Farquhar et al., 2003; Brunner and Bernasconi, 2005; Canfield et al., 2006), the magnitude of this sulfur isotope fractionation depends upon the isotope partitioning in each of the intercellular steps and on the ratio between the backward and forward sulfur fluxes within the bacterial cells (Rees, 1973; Brunner and Bernasconi, 2005).

Oxygen isotopes in sulfate, on the other hand, have been shown to be strongly influenced by the oxygen isotopic composition of water in which the bacteria are grown (e.g. Fritz et al., 1989; Brunner et al., 2005, 2012). The consensus is that, within the cell, sulfur compounds such as sulfite, and water exchange oxygen atoms; some of these isotopically equilibrated molecules return to the extracellular sulfate pool. As all the intercellular steps are considered to be reversible (Rees, 1973; Brunner and Bernasconi, 2005; Eckert et al., 2011; Holler et al., 2011), water-oxygen is also incorporated during the oxidation of these sulfur intermediates back to sulfate (Fritz et al., 1989; Brunner et al., 2006; Turchyn et al., 2006; Wortmann et al., 2007; Brunner et al., 2012; Antler et al., 2013; Wankel et al., 2013).

Thus, oxygen and sulfur isotopes in the residual sulfate during bacterial sulfate reduction are affected by the changes in the intercellular fluxes within the bacterial cells. However, these isotopes in the residual sulfate are affected in different ways, and therefore the relative change of one isotope vs. the other helps uniquely solve for the relative change in the flux of each intercellular step as sulfate is being reduced (Brunner et al., 2005, 2012; Antler et al., 2013). We term the relative changes in the fluxes at each intercellular step during bacterial sulfate reduction the 'mechanism' of bacterial sulfate reduction.

The sulfur and oxygen isotope composition of residual sulfate has been used to explore the mechanism of bacterial sulfate reduction during organic matter oxidation both in pure culture (e.g. Mangalo et al., 2007; Mangalo et al., 2008; Turchyn et al., 2010) and in the natural environment (e.g. Böttcher et al., 1998; Böttcher et al., 1999; Aharon and Fu, 2000, 2003; Turchyn et al., 2006; Wortmann et al., 2007; Antler et al., 2013). However, this isotope approach has not been used specifically to study sulfate-driven AOM, and to understand whether the intracellular mechanism of sulfate reduction is different when it is coupled to AOM as opposed to generic organic matter oxidation. This is partly because of the technical difficulty of measuring the isotopes of sulfate at the sulfate-methane transition, where the sulfate concentration is low.

In this study, we investigate sulfate-driven AOM at two different estuary sites using multi isotope measurements to further our understanding of the mechanism of this process. We report carbon isotopes in dissolved inorganic carbon ($\delta^{13}C_{DIC}$), sulfur and oxygen isotopes in pore fluid sulfate ($\delta^{34}S_{SO_4}$ and $\delta^{18}O_{SO_4}$ respectively) and carbon isotopes in pore fluid methane ($\delta^{13}C_{CH_4}$) as well as the concentrations of dissolved inorganic carbon, sulfate, and methane. Our samples were collected off the Mediterranean coast of Israel (The Yarqon and the Qishon estuaries, Fig. 1). The Yarqon is the largest coastal river in Israel with a length of 27.5 km and a drainage basin area of 1800 km^2. The estuary contains high organic carbon load from up-stream of 20–60 mg L^{-1} (Gafny et al., 2000) and a lower water mass close to seawater salinity. The Qishon stream drainage area occupies 1100 km^2, with intensive agricultural activity and industry taking place within the basin. The 7-km long Qishon estuary is characterized by the penetration of seawater, thereby producing a highly stratified water column. Nearby industrial plants provide high nutrients/carbon load in the Qishon estuary (Eliani-Russak et al., 2013). The salinity of the pore fluids in the two estuaries is close to the salinity of the eastern Mediterranean (Antler et al., 2013; Eliani-Russak et al., 2013) with a $\delta^{18}O_{H_2O}$ of 2 ± 0.5‰, similar to previous measurements of the $\delta^{18}O_{H_2O}$ of the eastern Mediterranean (e.g. Sisma-Ventura et al., 2009). Thus the water at the boundary layer of the estuary sediments is predominantly saline

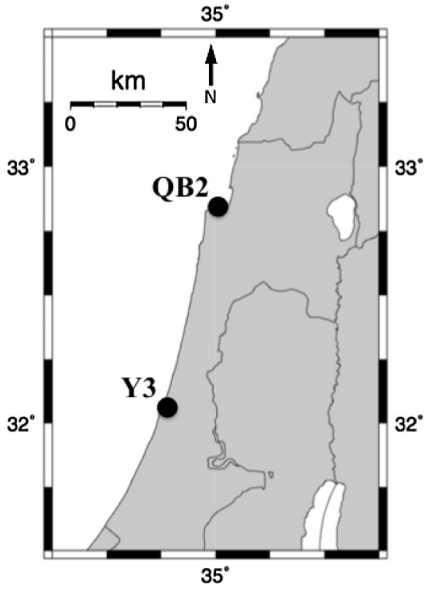

Fig. 1. Map of the study areas in a map of the Eastern Mediterranean region. The dots and the corresponding labels indicate the site locations and names, respectively.

Mediterranean water and the pore fluids see far less of the overlying freshwater. These two estuaries are ideal sites for our for studying the above mechanisms due to the high concentration of sulfate (seawater values of about 28 mM) and the high load of organic carbon, causing rapid depletion of sulfate within the sediments and intensive production of methane beneath.

2. Methods

2.1. Sampling and samples preparation

The sediments from the Yarqon estuary (location: 32° 4.334′N, 34°46.559′E, water depth: 2 m, distance from the shore: 1 km) were sampled by 50 cm long perspex tubes using a gravity corer. The sediments from the Qishon estuary (location: 32°48.503′N, 35°1.717′E; water depth: 4 m; distance from the shore: 0.7 km) were sampled by a box corer sub-sampled by 50 cm long Perspex tubes and by piston corer. The sediment was returned immediately to the lab and sliced to 1 cm slices under an argon atmosphere to avoid oxygen contamination. For methane and $\delta^{13}C_{CH_4}$ measurements, a special corer with side holes (1 cm in diameter) every 2 cm has been designed for quick and more precise subsampling. Through this special corer, ~2 ml of the sediment was taken using an edge cut syringe into a flushed argon bottle containing 5 ml sodium hydroxide (1.5 N) and the bottle was sealed with crimper.

Pore fluids were extracted using a centrifuge flushed with argon. 2 ml of filtered samples were transferred into vials for measurement of major ions and the $\delta^{18}O_{SO_4}$ and $\delta^{34}S_{SO_4}$. Those samples were flushed with argon for 15 min. Pore fluid sulfate was precipitated as barium sulfate (barite) using a saturated barium chloride solution. The barite was then washed with 6 N HCl and distilled water. For the DIC and $\delta^{13}C_{DIC}$ measurements the sample was filtered (0.45 μm) and transferred into poisoned syringe containing $HgCl_2$ powder.

2.2. Analytical methods

Sulfate concentrations were measured by High Performance Liquid Chromatography (HPLC, Dionex DX500) with an error of 3% between duplicates. DIC concentrations were measured according to the peak height and calibration curve on the Gas Source Isotopic Ratio Mass Spectrometer (GS-IRMS, Thermo) with an error of 0.2 mM 1 ml headspace sample was taken from the crimped vial with a gas-tight pressure lock after the bottle was shaken vigorously. Methane was measured from the headspace on a Focus Gas Chromatograph (Thermo) with ShinCarbon column with precision of 2 μM L^{-1}.

$\delta^{13}C_{DIC}$ and $\delta^{13}C_{CH_4}$ were measured by a Gas Source Isotopic Ratio Mass Spectrometer (GS-IRMS Thermo, at Ben Gurion University) through a Gas Bench II (GBII) interface and the PreCon (for $\delta^{13}C_{CH_4}$). The errors were 0.1‰ for $\delta^{13}C_{DIC}$ and 1‰ for $\delta^{13}C_{CH_4}$ between replicates. The values are reported vs. Vienna Pee Dee Belemnite (VPDB) standard.

For $\delta^{18}O_{SO_4}$ analysis, barite was pyrolyzed at 1450 °C in a Temperature Conversion Element Analyzer (TC/EA). The resulting carbon monoxide (CO) was measured by continuous helium flow on a GS-IRMS (Thermo Finnegan Delta V Plus, at the Godwin Laboratory, University of Cambridge). For the $\delta^{34}S_{SO_4}$ analysis, the barite was combusted at 1030 °C in a Flash Element Analyzer (EA), and the resulting sulfur dioxide (SO_2) was measured by continuous helium flow on a GS-IRMS (Thermo Finnegan Delta V Plus Godwin Laboratory, University of Cambridge). Samples for $\delta^{18}O_{SO_4}$ ran in replicates ($n = 3$–5) and the standard deviation of these replicate analyses was used as the error (~0.3‰ 1σ). The error for $\delta^{34}S_{SO_4}$ was determined using the standard deviation of the standard NBS 127 at the beginning and the end of each run (~0.3‰ 1σ). Samples for both $\delta^{18}O_{SO_4}$ and $\delta^{34}S_{SO_4}$ were corrected to NBS 127 ($\delta^{18}O_{SO_4}$ of 8.6‰ and $\delta^{34}S_{SO_4}$ of 20.3‰). The $\delta^{34}S_{SO_4}$ values are reported vs. Vienna Canyon Diablo Troilite (VCDT) and $\delta^{18}O_{SO_4}$ vs. Vienna Standard Mean Ocean water (VSMOW).

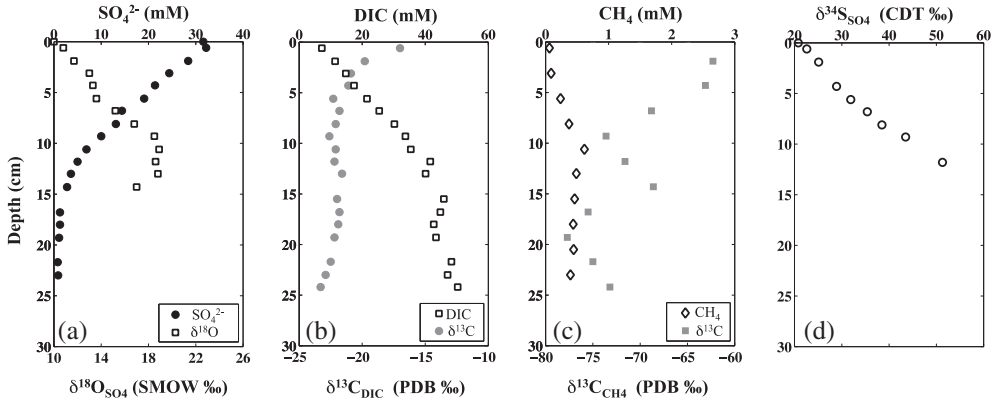

Fig. 2. Pore fluid profiles in the Yarqon estuary at sites Y3 of SO_4^{2-} and $\delta^{18}O_{SO_4}$ (a), DIC and $\delta^{13}C_{DIC}$ (b), CH_4 and $\delta^{13}C_{CH_4}$ (c) $\delta^{34}S_{SO_4}$ (d).

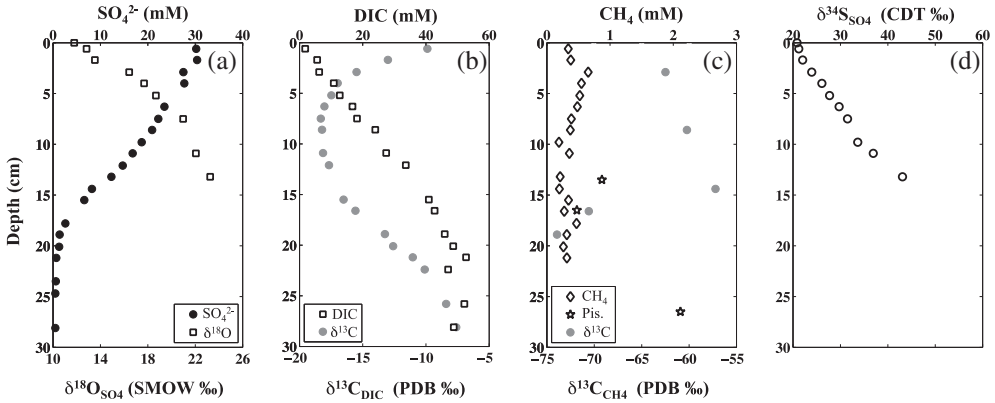

Fig. 3. Pore fluid profiles in the Qishon estuary at sites QB2 of SO_4^{2-} and $\delta^{18}O_{SO_4}$ (a), DIC and $\delta^{13}C_{DIC}$ (b), CH_4 and $\delta^{13}C_{CH_4}$ (c) $\delta^{34}S_{SO_4}$ (d). 'Pis' stand for samples that were taken from a piston corer.

3. Results

In the Yarqon estuary (Y3—Fig. 2) the pore-fluid sulfate concentration profile (Fig. 2a) shows an almost linear decrease from the sediment–water interface down to complete sulfate depletion at the sulfate-methane transition zone at 15 cm. The DIC concentration profile mirrors the sulfate profile, increasing from the sediment water interface to 50 mM at 25 cm (Fig. 2b). Methane concentrations increase from the sediment–water interface up to 0.6 mM around 11 cm depth and then level off (Fig. 2c). The $\delta^{13}C_{DIC}$ sharply decreases from −17‰ at the sediment–water interface to −23‰ at 10 cm and remains downcore at this value. Both the $\delta^{18}O_{SO_4}$ and $\delta^{34}S_{SO_4}$ increase with depth, below 10 cm the increase in $\delta^{18}O_{SO_4}$ moderates with depth (Fig. 2a and d, respectively). The $\delta^{13}C_{CH_4}$ values (Fig. 2c) are scattered throughout the core and vary over a range of around 15‰.

In the Qishon estuary (QB2—Fig. 3) sulfate is depleted by 18 cm. Similar to the profile observed in the Yarqon sediments, the DIC concentration profile mirrors the sulfate concentration profile. (Fig. 3a and b). Methane concentrations are similar in magnitude to the Yarqon in the box corer profile, however the piston corer profile enabled us to observe an increase in methane to 2 mM at a depth of 26 cm (Fig. 3c). In the Qishon the $\delta^{13}C_{DIC}$ decreases from −10‰ to −18‰ in the upper 10 cm, but then increases sharply to −7‰ by 30 cm (Fig. 3b). As in the Yarqon, in the Qishon both the $\delta^{18}O_{SO_4}$ and $\delta^{34}S_{SO_4}$ increase with depth (Fig. 4a and d, respectively). The $\delta^{13}C_{CH_4}$ data are scattered but shows 15‰ decrease below a depth of 15 cm (Fig. 3c).

4. Discussion

4.1. Methanogenesis and methanotrophy in the Yarqon and the Qishon sediments

At first glance, both studied sites seem to have comparable subsurface geochemistry and thus likely a similar sequence of anaerobic microbial reactions in the sediments: a decrease in sulfate concentrations and corresponding accumulation in DIC and some increase in methane concentrations (Figs. 2 and 3). Both sites are good candidates for sulfate-driven AOM in a marginal marine setting. Other than the depletion of sulfate followed by the increase in methane concentration, is there other evidence for both methane production and subsurface methane consumption in these estuarine environments?

One indication for methanogenesis and methanotrophy in these estuarine sediments is the $\delta^{13}C_{CH_4}$. During AOM, ^{12}C-bearing methane is preferentially oxidized leaving ^{13}C-bearing methane behind. Thus the $\delta^{13}C_{CH_4}$ should become more ^{12}C enriched with depth below the depth of methanotrophy due to less methane consumption and the production of ^{12}C enriched methane below.

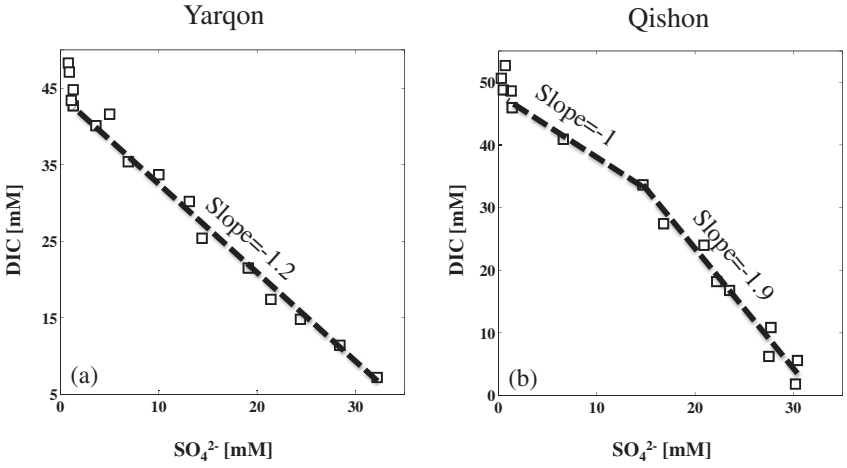

Fig. 4. DIC vs. sulfate concentration from the Yarqon (a) and the Qhison (b). The slope is −1.2 at the Yarqon whereas it is −1.9 at the Qishon in the upper part of the core and it decreases to −1 in the bottom part.

The $\delta^{13}C_{CH_4}$ profiles from the Yarqon and the Qishon cores suggest that at both sites there is subsurface methane production and consumption; $\delta^{13}C_{CH_4}$ increases from around −75‰ below the sulfate minimum zone to −60‰ in the top sediments (Figs. 2 and 3). This change in the $\delta^{13}C_{CH_4}$ suggests there is a zone of production of methane and above it a zone of consumption of methane. However, the scattered profiles do not allow us to estimate clearly the depth distribution.

The isotopic composition of DIC ($\delta^{13}C_{DIC}$) can also provide evidence for the spatial location of methanotrophy and methanogenesis within subsurface sediments. Due to the extremely high carbon isotope fractionation during methanogenesis (up to 100‰—Whiticar, 1999) the resulted methane is much more ^{12}C enriched, or lighter, than the resulting or residual DIC. Methane oxidation, on the other hand, has a much smaller carbon isotope fractionation (0–10‰—Alperin et al., 1988; Martens et al., 1999), producing DIC that has a similar carbon isotope composition to its methane precursor. The $\delta^{13}C_{DIC}$ profiles from the Yarqon and the Qishon (Figs. 2b and 3b, respectively) are markedly different, although from the sediment–water interface to 7 cm depth the $\delta^{13}C_{DIC}$ decreases at both of the cores, suggesting ^{12}C enriched DIC is being added to the pore fluids. However, below 7 cm in the Yarqon, the $\delta^{13}C_{DIC}$ remains fairly constant (Fig. 2b) while in the Qishon the $\delta^{13}C_{DIC}$ starts to increase again, as would be expected from the classic isotope geochemistry profiles of in situ deep methanogenesis (Fig. 3b).

The fact that the $\delta^{13}C_{DIC}$ in the Yarqon does not increase suggests that the methane is produced much further below the studied core or that the methane is produced and consumed at the same depth (7 cm in the Yarqon). If the methane is produced below the studied sediment core, then at this 'other location' a pool of isotopically heavy DIC would exist, coupled to the isotopically light pool of generated methane. That isotopically heavy DIC would need to be diffusing elsewhere, or precipitated as authigenic carbonate at the 'other location' such that we do not observe it within our studied sediment core, while the methane diffuses to our studied site. The second possibility to explain the lack of change in the $\delta^{13}C_{DIC}$ below 7 cm in the Yarqon is that the methane is produced at the same depth where it is consumed. This would create an isotopically closed system where the $\delta^{13}C_{DIC}$ does not change dramatically. This is consistent with the measurement of isotopically light methane that we have produced in the Yarqon. Since methane concentrations are 2 order of magnitude less than the DIC concentration, ^{12}C-rich methane can be generated (in small concentration) without necessarily impacting the residual $\delta^{13}C_{DIC}$.

The difference in the $\delta^{13}C_{DIC}$ profiles between the Qishon and the Yarkon is the first suggestion that the subsurface microbial processes are different between these two sites. While the carbon isotopes suggest that the location of methanogenesis and methanotrophy are different between the Yarqon and Qishon estuaries, our question is whether this impacts the link between sulfate and methane. The sulfate concentration profiles at both sites are slightly different as well. While at the Yarqon site the sulfate concentration profile is almost linear, at the Qishon site the sulfate concentration profile is slightly concave-up. We plot the DIC vs. SO_4 concentrations (Fig. 4), which reveal that the ratio of change in sulfate vs. DIC is also different between the sites. In the Yarqon sediments, the ratio of change in sulfate vs. DIC is close to −1:1 (1 mol of sulfate consumed to 1 mol of DIC generated Fig. 4a), while in the Qishon estuary the ratio is not constant with depth and changes from almost −1:2 at the upper part of the core to −1:1 at the lower part (Fig. 4b). This stoichiometric ratio between sulfate and DIC hints at the pathway through which sulfate is being consumed: during sulfate-driven AOM we expect a ratio of −1:1 (Similar to Burdige and Komada, 2011) between sulfate consumption and DIC production (Eq. (1), introduction), while in organic matter oxidation we expect a mol ratio of −1:2 for sulfate consumption to DIC production:

$$SO_4^{2-} + 2CH_2O \rightarrow 2HCO_3^- + H_2S \quad (2)$$

This stoichiometry by itself, however, does not provide definitive evidence for the microbial processes occurring in these sediments. This is because there might be other sources and sinks of DIC (or sulfate) in the sediment that could interfere with the stoichiometrically predicted ratios. For example, oxidation of organic matter by electron acceptors other than sulfate, or precipitation of carbonate minerals could both interfere with the ratio of sulfate to DIC. Furthermore, subsurface sulfide oxidation could also interfere with the sulfate-DIC ratio. Although these may be a problem in this environment, we still conclude that the sharply different sulfate-to-DIC ratios between the sites indicate sulfate-driven AOM dominates in the Yarqon sediments and in the Qishon, the upper 10 cm are dominated by organo-clastic sulfate reduction and sulfate-driven AOM is occurring below.

Over all, although there are similarities in the concentration profiles of pore fluid sulfate, DIC and the methane concentrations between the Yarqon and Qishon estuary sites, the rate of change of the sulfate vs. DIC and the carbon isotopes (of both methane and DIC) are fundamentally different. We suggest that these differences can be attributed to different depth distributions of the microbial activity or to the reactivity of organic matter. In the Qishon, the microbial activity is spatially stacked like the 'classic' marine sulfate-driven AOM profiles, with the upper section (0–7 cm) dominated by sulfate-driven organic matter oxidation, the middle section (7–15 cm) dominated by sulfate-driven AOM and the bottom section (15–30 cm) dominated by methanogenesis (Figs. 2 and 3). In contrast, in the Yarqon, the methane is either being produced and consumed at the same depth or is being produced elsewhere and is diffusing into the studied core, and there is little evidence that sulfate is consumed through anything other than sulfate-driven AOM.

4.2. Sulfur and oxygen isotope insight into the sulfate-methane coupling

As suggested above, the pore fluid profile of DIC and sulfate do not, alone, provide enough detail about the mechanism of sulfate-driven AOM in either the Yarqon or Qishon sediments. In contrast the carbon isotopes of the DIC suggest that the distribution of methane production and consumption may be different at the two sites. Given that we have the potential for different processes between these two sites, the question is whether we see a difference in the mechanism of sulfate reduction between these two sites. As mentioned in the introduction, the sulfur and oxygen isotope composition of pore fluid sulfate can yield unique insight into our understanding of the mechanism of sulfate reduction when coupled either to organic matter oxidation or to AOM.

Although both the sulfur and oxygen isotope composition of sulfate increase at both sites, the relative change in the $\delta^{18}O_{SO_4}$ vs. $\delta^{34}S_{SO_4}$ is unique at each site, hinting that the mechanism of sulfate reduction differs between the different sulfate-driven AOM zones (Fig. 5). The $\delta^{18}O_{SO_4}$ vs. $\delta^{34}S_{SO_4}$ cross-plot from the Yarqon shows two stages; until 10 cm depth the $\delta^{18}O_{SO_4}$ increases moderately relative to the $\delta^{34}S_{SO_4}$ (=0.37—Fig. 5a), but deeper in the sediment the $\delta^{18}O_{SO_4}$ remains constant while $\delta^{34}S_{SO_4}$ increases. At the Qishon the slope between the $\delta^{18}O_{SO_4}$ and $\delta^{34}S_{SO_4}$ is almost double that of the Yarqon, but becomes more moderate at depth (Fig. 5a—solid line). However, due to poor sampling resolution (low sulfate concentration yields small amount of barite which is then not sufficient

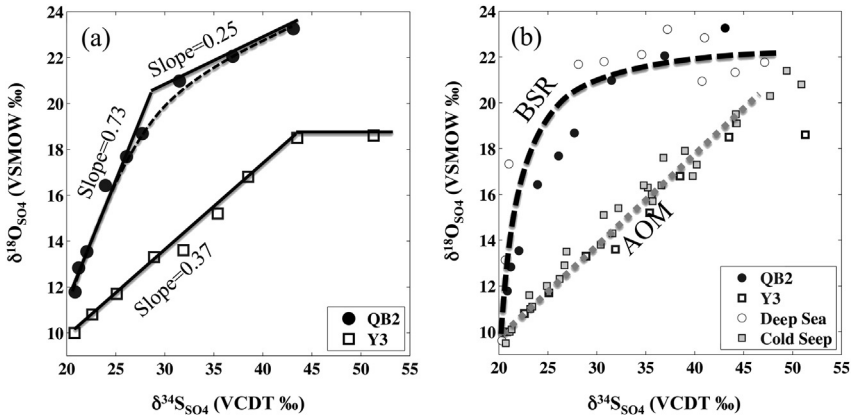

Fig. 5. $\delta^{18}O_{SO_4}$ vs. $\delta^{34}S_{SO_4}$ from the Yarqon (site Y3-opened squares) and the Qishon (site QB2-closed circles) estuaries (Israel), the solid lines are tow-stages linear fit, and the dashed line is the option of concaved curve (a), and data from Organic-carbon poor deep-sea sediment (Turchyn et al., 2006) and cold seeps (Aharon and Fu, 2000). The dashed lines are schematic. BSR stands for bacterial sulfate reduction.

for $\delta^{18}O_{SO_4}$ and $\delta^{34}S_{SO_4}$ analysis), we suggest that the moderation of the slope in the Qishon may actually be concave, as has been seen at other sites (e.g. Böttcher et al., 1998; Aller et al., 2010; Antler et al., 2013) and not necessarily a two-step curve (Fig. 5a-dashed line).

Extending this type of dataset to other sulfate-methane transition zones would allow us to probe how different mechanisms of sulfate-driven AOM are manifest in subsurface isotope geochemistry. However, the paucity of isotope data from similar marginal marine environments makes this comparison tricky. The slope of $\delta^{18}O_{SO_4}$ vs. $\delta^{34}S_{SO_4}$ seems to be pointing to environmental controls on the mechanism of sulfate reduction. For example, Aharon and Fu (2000) studied the relationship between $\delta^{18}O_{SO_4}$ and $\delta^{34}S_{SO_4}$ in the Gulf of Mexico and found that the slope emerging between $\delta^{18}O_{SO_4}$ vs. $\delta^{34}S_{SO_4}$ is as low as 0.29 during sulfate reduction associated with gas seeps. Values for the slope in the $\delta^{18}O_{SO_4}$ vs. $\delta^{34}S_{SO_4}$ cross plot that are as low as this have been recently observed also by Rubin-Blum et al. (2014) in gas seeps off the shore of Israel. On the other hand, in natural environments where no methane was detected and bacterial sulfate reduction proceeds via organo-clastic oxidation, the slope between $\delta^{18}O_{SO_4}$ vs. $\delta^{34}S_{SO_4}$ is normally steeper than 0.8 (compiled by Antler et al., 2013). We plot these two extremes of the slope of $\delta^{18}O_{SO_4}$ vs. $\delta^{34}S_{SO_4}$ together with data from the current study (Fig. 5b): We used the data from Turchyn et al. (2006) (ODP site 1086, leg 175, located in the West African Margin in 780 m deep water) as a representative of an organo-clastic sulfate reduction dominated site, and the data from Aharon and Fu (2000) (located in the Gulf of Mexico, water depth of 591 m) as representative of a site where sulfate-driven AOM dominates. Note that the $\delta^{18}O_{SO_4}$ data that were taken from Aharon and Fu (2000) were recorrected to the current value of seawater (8.6‰) as opposed to 9.6‰ that was used at that time so that they can be compared to the rest of the literature data. The circles on the furthest left represent bacterial sulfate reduction only through organic matter oxidation (the data is from an organic carbon-poor deep-sea sediment site) while the squares are the data from the gas seep in the Gulf of Mexico (Aharon and Fu, 2000). Our data fall between these extremes, however the data from the Qishon are closer to the organic-carbon-poor deep-sea sediment site and the data from the Yarqon are more similar in slope to the gas seep site with dominated sulfate-driven AOM.

The shape of the $\delta^{18}O_{SO_4}$ vs. $\delta^{34}S_{SO_4}$ cross-plot holds information about the recycling of sulfur intermediates during bacterial sulfate reduction, as discussed in the introduction (Brunner et al., 2005; Turchyn et al., 2006; Wortmann et al., 2007; Brunner et al., 2012; Antler et al., 2013). The quicker the $\delta^{18}O_{SO_4}$ changes relative to $\delta^{34}S_{SO_4}$ (or the steeper the slope on a cross plot like in Fig. 5) the more sulfate is brought into the cell, exchanges oxygen atoms with water, and is returned back to the extracellular sulfate pool, relative to the amount that is reduced (Antler et al., 2013). In contrast, when the $\delta^{34}S_{SO_4}$ evolves more rapidly than the $\delta^{18}O_{SO_4}$ (a shallower slope on a cross plot like Fig. 5), then more sulfate is brought into the cell and reduced, and less is intercellularly recycled back to sulfate. Changes in the slope of the isotopes in $\delta^{18}O_{SO_4}$ vs. $\delta^{34}S_{SO_4}$ space likely indicate changes in the mechanism of which sulfate is been reduced (changes in the intercellular forward and backward fluxes).

There are other factors that can impact the relationship between $\delta^{18}O_{SO_4}$ and $\delta^{34}S_{SO_4}$ that may be important within these estuary sediments. For example anaerobic sulfide oxidation within marine sediments would produce sulfate that has a low $\delta^{34}S_{SO_4}$ and a $\delta^{18}O_{SO_4}$ close to the $\delta^{18}O$ of the water (e.g. Aller et al., 2010); this would drive the uppermost pore fluids both lower in their sulfur and oxygen isotope compositions. Also, if sulfide is partially reoxidized and then undergoes disproportionation this would also impact the slope of $\delta^{18}O_{SO_4}$ vs. $\delta^{34}S_{SO_4}$, although this would have a variable effect on the isotopes given the pathway of disproportionation (Cypionka et al., 1998; Böttcher et al., 2001, 2005; Böttcher and Thamdrup, 2001; Aharon and Fu, 2003). We assume that these processes are less important in these estuary sediments than the dominant process of sulfate-driven AOM. In addition, if the sulfate concentration is not in steady state, as the sulfate concentration profile in the Qishon may suggest, this can impact the relationship between $\delta^{18}O_{SO_4}$ and $\delta^{34}S_{SO_4}$. Aller et al. (2010) has shown that the impact of the non-steady state sulfate concentrations on the $\delta^{18}O_{SO_4}$ vs. $\delta^{34}S_{SO_4}$ is not dramatic. In addition, in the Qishon and the Yarqon, the characteristic time scale of diffusion of sulfate is at least an order of magnitude higher than in the sediment that Aller et al. (2010) studied and therefore the $\delta^{18}O_{SO_4}$ vs. $\delta^{34}S_{SO_4}$ relationship should be much more resilient to perturbations in sulfate concentration. Finally, the uppermost pore water consists mainly of seawater at both sites with similar oxygen isotopic composition of the water. This rules out that the difference between the two sites is a result of a different water source.

For these two estuaries, we suggest that as the slope of $\delta^{18}O_{SO_4}$ vs. $\delta^{34}S_{SO_4}$ decreases with depth at both studied sites this indicates a shift in the mechanism of bacterial sulfate reduction (Fig. 5a). In the Yarqon, where this moderation is not linked to other geochemical changes with depth in the core, we suggest that this moderation may reflect a subtle change of the percentage of recycling of sulfur intermediates, or the point where the oxygen

isotopes have reached 'apparent equilibrium' with water. On the other hand, in the Qishon, the change in the slope of the $\delta^{18}O_{SO_4}$ vs. $\delta^{34}S_{SO_4}$ cross-plot is synchronous with the break in slope in DIC:-sulfate space (Fig. 4) and the change in the carbon isotopes of pore fluid DIC. This suggests that the sulfur and oxygen isotopes in sulfate shift in the Qishon in response to a change in the type of the electron donor used by the sulfate reducing bacteria from organic matter to methane. The reason for this difference in the mechanism of the sulfate reduction may be connected to the depositional setting of each of the site. We speculate, that the high organic content (TOC) in the Qishon (~10%) vs. the Yarqon (~2.5%) may promote organo-clastic sulfate reduction over sulfate-driven AOM (Sivan et al., 2007; Pohlman et al., 2013) at the upper part of the sediment.

Recent studies have found that the pathway by which sulfate is being reduced during sulfate-driven AOM may be fundamentally different than during bacterial sulfate reduction (Holler et al., 2011; Milucka et al., 2012). During sulfate-driven AOM, zero-valent sulfur was found to be a key intermediate, which later can be disproportionated resulting in sulfide and sulfate (Milucka et al., 2012). The impact of this fundamentally different mechanism on the $\delta^{18}O_{SO_4}$ vs. $\delta^{34}S_{SO_4}$ is not yet clear. Steeper $\delta^{18}O_{SO_4}$ vs. $\delta^{34}S_{SO_4}$ is typically correlated to higher percentage of recycling of sulfur intermediates (Brunner et al., 2005, 2012; Antler et al., 2013). Our results suggest that during sulfate-driven AOM, less sulfur intermediates are being re-oxidized back to sulfate compared to organo-clastic sulfate reduction.

Another possibility is that the linear trend found in the $\delta^{18}O_{SO_4}$ vs. $\delta^{34}S_{SO_4}$ cross plot at sites with sulfate-driven AOM is a result of mixing through diffusion of sulfate with two isotopic end members. This explanation however has been challenged due to the different environmental setting of the sediments from the Yarqon estuary and the Gulf of Mexico, with significantly different temperature, porosity, water pressure and sedimentation rate, which impact the rate of diffusion of sulfate and is different isotopologues.

5. Summary and conclusions

In this study we present pore fluid isotopes and concentration measurements from two estuaries, the Yarqon and the Qishon. These pore fluid profiles show steep redox gradients, including depletion of sulfate concentration with depth and a corresponding increase in the concentrations of DIC and methane. Although these two estuaries are similar in many regards, the zonation of various processes differs between the two sites. Our data indicate that in the Qishon, organo-clastic sulfate reduction takes place in the upper part of the sediment and sulfate-driven AOM occurs below. In contrast, at the Yarqon, the entire sediment is mostly dominated by sulfate-driven AOM. We suggest that the use of multiple isotopic and geochemical measurements elucidate these differences.

In addition, the $\delta^{18}O_{SO_4}$ vs. $\delta^{34}S_{SO_4}$ pattern at these two sites is different; this suggests different pathways for the sulfate to be reduced and recycled. Our new data, together with data from the literature reveals that the $\delta^{18}O_{SO_4}$ vs. $\delta^{34}S_{SO_4}$ for the Qishon is similar to sites from organic-carbon poor deep-sea sediments where organo-clastic is dominates, whereas the Yarqon is similar to cold seeps, which are dominated by sulfate-driven AOM. We suggest that the different $\delta^{18}O_{SO_4}$ vs. $\delta^{34}S_{SO_4}$ patterns are the result of different mechanisms during this processes. However experiments with natural sediments are required to rule out the effect of diffusion or advection that may result in linear correlation between $\delta^{18}O_{SO_4}$ vs. $\delta^{34}S_{SO_4}$ in cold seeps. These patterns have the potential to provide a unique geochemical fingerprint for each process, and therefore aid us in assessing the location of these processes within marine or marginal marine sediments. In addition, this fingerprint could potentially be preserved in the geological record in the form of carbonate-associated sulfate particularly in authigenic carbonates. Further research is needed to tie the mechanism of sulfate-driven AOM and its $\delta^{18}O_{SO_4}$ vs. $\delta^{34}S_{SO_4}$ fingerprint.

Acknowledgments

We are grateful to Dr. D. Pargament and P. Rubinzaft from the Yarkon River Authority and to the crew of the R/V Shikmona from the Israel Oceanographic and Limnological Research Institute (IOLR) for their technical support in the field. We are in debt with E. Eliani-Russak from Ben Gurion University of the Negev and with J. Rolfe from the Godwin Laboratory at the University of Cambridge for their technical support in the laboratory. We are thankful to Prof. G. Jiwchar for the use in the HPLC. We would like to thank the two anonymous reviewers that, with their comments, helped improve the final version of this manuscript. Field assistance was provided by M. Adler, T. Bishop, N. Knossow and E. Woodward. G. Antler would like to thanks S. Povia, A. Russak, N. Avrahamov, I. Bar-Or and E. Levy for assistance in different aspects of this manuscript.

G. Antler is supported by the Cambridge Overseas Trust. This research was supported by the British Council BIRAX grant BY2/GEO/04 jointly to AVT and OS and the Israel Science Foundation (#643/12).

Appendix A. Supplementary data

Supplementary data related to this article can be found at http://dx.doi.org/10.1016/j.ecss.2014.03.001.

References

Aharon, P., Fu, B., 2000. Microbial sulfate reduction rates and sulfur and oxygen isotope fractionations at oil and gas seeps in deepwater Gulf of Mexico. Geochim. Cosmochim. Acta 64 (2), 233–246.

Aharon, P., Fu, B., 2003. Sulfur and oxygen isotopes of coeval sulfate–sulfide in pore fluids of cold seep sediments with sharp redox gradients. Chem. Geol. 195 (1), 201–218.

Alperin, M.J., Reeburgh, W.S., Whiticar, M.J., 1988. Carbon and hydrogen isotope fractionation resulting from anaerobic methane oxidation. Glob. Biogeochem. Cycles 2 (3), 279–288.

Aller, R.C., Madrid, V., Chistoserdov, A., Aller, J.Y., Heilbrun, C., 2010. Unsteady diagenetic processes and sulfur biogeochemistry in tropical deltaic muds: implications for oceanic isotope cycles and the sedimentary record. Geochim. Cosmochim. Acta 74, 4671–4692.

Antler, G., Turchyn, A.V., Rennie, V., Herut, B., Sivan, O., 2013. Coupled sulfur and oxygen isotope insight into bacterial sulfate reduction in the natural environment. Geochim. Cosmochim. Acta 118, 98–117.

Barnes, R.O., Goldberg, E.D., 1976. Methane production and consumption in anoxic marine sediments. Geology 4 (5), 297–300.

Blair, N.E., Aller, R.C., 1995. Anaerobic methane oxidation in Amazon shelf sediments. Geochim. Cosmochim. Acta 59, 3707–3715.

Boetius, A., Ravenschlag, K., Schubert, C.J., Rickert, D., Widdel, F., Gieseke, A., Amann, R., Jørgensen, B.B., Witte, U., Pfannkuche, O., 2000. A marine microbial consortium apparently mediating anaerobic oxidation of methane. Nature 407 (6804), 623–626.

Borowski, W.S., Hoehler, T.M., Alperin, M.J., Rodriguez, N.M., Paull, C.K., 2000. Significance of anaerobic methane oxidation in methane-rich sediments overlying the Blake Ridge gas hydrates. Proc. Ocean Drill Prog. Sci. Results 164, 87–99.

Böttcher, M.E., Thamdrup, B., 2001. Anaerobic sulfide oxidation and stable isotope fractionation associated with bacterial sulfur disproportionation in the presence of MnO_2. Geochim. Cosmochim. Acta 65, 1573–1581.

Böttcher, M.E., Brumsack, H.J., de Lange, G.J., 1998. Sulfate reduction and related stable isotope (^{34}S, ^{18}O) variations in interstitial waters from the eastern Mediterranean. Proc. Ocean Drill Prog. Sci. Results 160, 365–373.

Böttcher, M.E., Bernasconi, S.M., Brumsack, H.J., 1999. Carbon, sulfur, and oxygen isotope geochemistry of interstitial waters from the western Mediterranean. Proc. Ocean Drill Prog. Sci. Results 161, 413–421.

Böttcher, M.E., Thamdrup, B., Vennemann, T.W., 2001. Oxygen and sulfur isotope fractionation during anaerobic bacterial disproportionation of elemental sulfur. Geochim. Cosmochim. Acta 65, 1601–1609.

Brunner, B., Bernasconi, S.M., 2005. A revised isotope fractionation model for dissimilatory sulfate reduction in sulfate. Geochim. Cosmochim. Acta 69 (20), 4759–4771.

Brunner, B., Bernasconi, S.M., Kleikemper, J., Schroth, M.J., 2005. A model for oxygen and sulfur isotope fractionation in sulfate during bacterial sulfate reduction processes. Geochim. Cosmochim. Acta 69, 4773–4785.
Brunner, B., Einsiedl, F., Arnold, G.L., Müller, I., Templer, S., Bernasconi, S.M., 2012. The reversibility of dissimilatory sulphate reduction and the cell-internal multi-step reduction of sulphite to sulphide: insights from the oxygen isotope composition of sulphate. Isotopes Environ. Health Stud. 48 (1), 33–54.
Burdige, D.J., Komada, T., 2011. Anaerobic oxidation of methane and the stoichiometry of remineralization processes in continental margin sediments. Limnology Oceanogr. 56 (5), 1781–1796.
Canfield, D.E., Olesen, C.A., Cox, R.P., 2006. Temperature and its control of isotope fractionation by a sulfate-reducing bacterium. Geochim. Cosmochim. Acta 70, 548–561.
Cicerone, R.J., Oremland, R.S., 1998. Biogeochemical aspects of atmospheric methane. Global Biogeochem. Cycles 2 (4), 299–327.
Cypionka, H., Smock, A., Böttcher, M.E., 1998. A combined pathway of sulfur compound disproportionation in Desulfovibrio desulfuricans. FEMS Microbiol. Lett. 166, 181–186.
Eckert, T., Brunner, B., Edwards, E.A., Wortmann, U.G., 2011. Microbially mediated re-oxidation of sulfide during dissimilatory sulfate reduction by Desulfobacter latus. Geochim. Cosmochim. Acta 75, 3469–3485.
Eliani-Russak, E., Herut, B., Sivan, O., 2013. The role of highly sratified nutrient-rich small estuaries as a source of dissolved inorganic nitrogen to coastal seawater, the Qishon (SE Mediterranean) case. Mar. Pollut. Bull. 71, 250–258.
Farquhar, J., Johnston, D.T., Wing, B.A., Habicht, K.S., Canfield, D.E., Airieau, S., Thiemens, M.H., 2003. Multiple sulphur isotopic interpretations of biosynthetic pathways: implications for biological signatures in the sulphur isotope record. Geobiology 1, 27–36.
Fritz, P., Basharmal, G.M., Drimmie, R.J., Ibsen, J., Qureshi, R.M., 1989. Oxygen isotope exchange between sulfate and water during bacterial reduction of sulfate. Chem. Geol. 79, 99–105.
Froelich, P., Klinkhammer, G., Bender, M., Luedtke, N., Heath, G.R., Cullen, D., Dauphin, P., Hammond, D., Hartman, B., Maynard, V., 1979. Early oxidation of organic matter in pelagic sediments of the eastern equatorial Atlantic: suboxic diagenesis. Geochim. Cosmochim. Acta 43, 1075–1090.
Gafny, S., Goren, M., Gasith, A., 2000. Habitat condition and fish assemblage structure in a coastal Mediterranean stream (Yarqon, Israel) receiving domestic effluent. In: Jungwirth, M., Muhar, S., Schmutz, S. (Eds.), Assessing the Ecological Integrity of Running Waters Developments in Hydrobiology. Springer, Dordrecht, Netherlands, pp. 319–330.
Hinrichs, K.U., Hayes, J.M., Sylva, S.P., Brewer, P.G., DeLong, E.F., 1999. Methane-consuming archaebacteria in marine sediments. Nature 398 (6730).
Hoehler, T.M., Alperin, M.J., Albert, D.B., Martens, C.S., 1994. Field and laboratory studies of methane oxidation in an anoxic marine sediment: evidence for a methanogen-sulfate reducer consortium. Glob. Biogeochem. Cycles 8 (4), 451–463.
Holler, T., Wegener, G., Niemann, H., Deusner, C., Ferdelman, T.G., Boetius, A., Brunner, B., Widdel, F., 2011. Carbon and sulfur back flux during anaerobic microbial oxidation of methane and coupled sulfate reduction. Proc. Natl. Acad. Sci. U S A 108 (52), 1484–1490.
Kasten, S., Jørgensen, B.B., 2000. Sulfate reduction in marine sediments. In: Schulz, H.D., Zabel, M. (Eds.), Marine Geochemistry. Springer, Berlin, Heidelberg, pp. 263–281.
Kvenvolden, K.A., 1988. Methane hydrate—a major reservoir of carbon in the shallow geosphere? Chem. Geol. 71 (1), 41–51.
Malinverno, A., Pohlman, J.W., 2011. Modeling sulfate reduction in methane hydrate-bearing continental margin sediments: does a sulfate-methane transition require anaerobic oxidation of methane? Geochem. Geophys. Geosys. 12, Q07006.
Martens, C.S., Berner, R.A., 1974. Methane production in the interstitial waters of sulfate-depleted marine sediments. Sci. (N.Y.) 185 (4157), 1167–1169.
Martens, C.S., Albert, D.B., Alperin, M.J., 1999. Stable isotope tracing of anaerobic methane oxidation in the gassy sediments of Eckernforde Bay, German Baltic Sea. Am. J. Sci. 299 (7–9), 589–610.
Milucka, J., Ferdelman, T.G., Polerecky, L., Franzke, D., Wegener, G., Schmid, M., Lieberwirth, I., Wagner, M., Widdel, Kuypers, M.M.M., 2012. Zero-valent sulphur is a key intermediate in marine methane oxidation. Nature 491 (7425), 541–546.
Mangalo, M., Meckenstock, R.U., Stichler, W., Einsiedl, F., 2007. Stable isotope fractionation during bacterial sulfate reduction is controlled by reoxidation of intermediates. Geochim. Cosmochim. Acta 71, 4161–4171.
Mangalo, M., Einsiedl, F., Meckenstock, R.U., Stichler, W., 2008. Influence of the enzyme dissimilatory sulfite reductase on stable isotope fractionation during sulfate reduction. Geochim. Cosmochim. Acta 71, 4161–4171.
Niemann, H., Lösekann, T., de Beer, D., Elvert, M., Nadalig, T., Knittel, K., Amann, R., Sauter, E.J., Schlüter, M., Klages, M., Foucher, J.P., Boetius, A., 2006. Novel microbial communities of the Haakon Mosby mud volcano and their role as a methane sink. Nature 443 (7113), 854–858.
Niewöhner, C., Hensen, C., Kasten, S., Zabel, M., Schulz, H.D., 1998. Deep sulfate reduction completely mediated by anaerobic methane oxidation in sediments of the upwelling area off Namibia. Geochim. Cosmochim. Acta 62 (3), 455–464. Chicago.
Orphan, V.J., House, C.H., Hinrichs, K.U., McKeegan, K.D., DeLong, E.F., 2001. Methane-consuming archaea revealed by directly coupled isotopic and phylogenetic analysis. Sci. (N.Y.) 293 (5529), 484–487.
Orphan, Victoria J., House, C.H., Hinrichs, K.-U., McKeegan, K.D., DeLong, E.F., 2002. Multiple archaeal groups mediate methane oxidation in anoxic cold seep sediments. Proc. Natl. Acad. Sci. U S A 99 (11), 7663–7668.
Pohlman, J.W., Riedel, M., Bauer, J.E., Canuel, E.A., Paull, C.K., Lapham, L., Grabowski, K.S., Coffin, R.B., Spence, G.D., 2013. Anaerobic methane oxidation in low-organic content methane seep sediments. Geochim. Cosmochim. Acta 108, 184–201.
Reeburgh, W.S., 1976. Methane consumption in Cariaco trench waters and sediments. Earth Planet. Sci. Lett. 28 (3), 337–344.
Reeburgh, W.S., 2007. Oceanic methane biogeochemistry. Chem. Rev. 107, 486–513.
Rees, C.E., 1973. A steady-state model for sulphur isotope fractionation in bacterial reduction processes. Geochim. Cosmochim. Acta 37 (5), 1141–1162.
Rubin-Blum, M., Antler, G., Turchyn, A.V., Tsadok, R., Goodman-Tchernov, B.N., Shemesh, E., Austin, J.A., Coleman, D.F., Makovsky, Y., Sivan, O., Tchernov, D., 2014. Hydrocarbon-related microbial processes in the deep sediments of the Eastern Mediterranean Levantine Basin. FEMS Microbiol. Ecol. 87, 780–796. http://dx.doi.org/10.1111/1574-6941.12264.
Sisma-Ventura, G., Guzner, B., Yam, R., Fine, M., Shemesh, A., 2009. The reef builder Dendropoma petraeum—a proxy of short and long term climatic events in the eastern Mediterranean. Geochim. Cosmochim. Acta 73, 4376–4383.
Sim, M.S., Bosak, T., Ono, S., 2011. Large sulfur isotope fractionation does not require disproportionation. Science 333, 74–77.
Sivan, O., Schrag, D.P., Murray, R.W., 2007. Rates of methanogenesis and methanotrophy in deep-sea sediments. Geobiology 5 (2), 141–151.
Turchyn, A.V., Sivan, O., Schrag, D., 2006. Oxygen isotopic composition of sulfate in deep sea pore fluid: evidence for rapid sulfur cycling. Geobiology 4, 191–201.
Turchyn, A.V., Brüchert, V., Lyons, T.W., Engel, G.S., Balci, N., Schrag, D.P., Brunner, B., 2010. Kinetic oxygen isotope effects during dissimilatory sulfate reduction: a combined theoretical and experimental approach. Geochim. Cosmochim. Acta 74, 2011–2024.
Wankel, S.D., Bradley, A.S., Eldridge, D.L., Johnston, D.T., 2013. Determination and application of the equilibrium oxygen isotope effect between water and sulfite. Geochim. Cosmochim. Acta 125, 694–711.
Whiticar, M.J., Faber, E., Schoell, M., 1986. Biogenic methane formation in marine and freshwater environments: CO_2 reduction vs. acetate fermentation—isotope evidence. Geochim. Cosmochim. Acta 50 (5), 693–709.
Whiticar, M.J., 1999. Carbon and hydrogen isotope systematics of bacterial formation and oxidation of methane. Chem. Geol. 161 (1–3), 291–314.
Wortmann, U.G., Bernasconi, S.M., Böttcher, M.E., 2001. Hypersulfidic deep biosphere indicates extreme sulfur isotope fractionation during single-step microbial sulfate reduction. Geology 29, 647–650.
Wortmann, U.G., Chernyavsky, B., Bernasconi, S.M., Brunner, B., Böttcher, M.E., Swart, P.K., 2007. Oxygen isotope biogeochemistry of pore water sulfate in the deep biosphere: dominance of isotope exchange reactions with ambient water during microbial sulfate reduction (ODP Site 1130). Geochim. Cosmochim. Acta 71 (17), 4221–4232.
Wuebbles, D., Hayhoe, K., 2002. Atmospheric methane and global change. Earth-Sci. Rev. 57 (3–4), 177–210.